THE JOURNAL OF PHYSICAL CHEMISTRY B

ARTICLE

pubs.acs.org/JPCB

Rotational Diffusion Analysis of Polyethylene Glycol Induced Protein Interactions

Daisuke Takahashi,[†,‡] Shoji Yamashita,[†] Om Prakash,[‡] and Etsuko Nishimoto*[,†]

[†]Institute of Biophysics, Faculty of Agriculture, Kyushu University, 6-10-1 Hakozaki, Higashi-ku, Fukuoka 812-8581, Japan

[‡]Department of Biochemistry, Kansas State University, Manhattan, Kansas 66506, United States

ABSTRACT: Protein intermolecular depletion interactions induced by polyethylene glycol (PEG) depend largely on its concentration and molecular weight. Herein, we investigated the effects of various concentrations and molecular weights of PEG on lysozyme interactions through the analysis of protein rotational diffusion, which is susceptible to intermolecular interactions at short range. To this end, we measured fluorescence anisotropy of fluorescein-tagged lysozyme added as a tracer in concentrated native lysozyme solutions and introduced a protein concentration-dependent interaction parameter, k_{rot}. The results show the nonmonotonic changes in k_{rot} as the concentrations of PEG10000 and 6000 are increased. The depletion attractions are characterized by the decrease in k_{rot}, indicating an increase of a degree at which protein rotational diffusion slows down. The influences of temperature on the lysozyme rotational diffusion and k_{rot} were also measured, and the validity of this approach was checked through comparison with the colloidal theory.

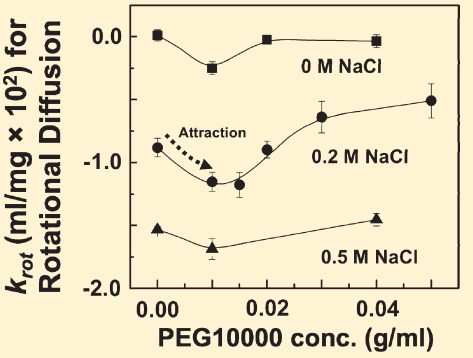

INTRODUCTION

Polyethylene glycol (PEG) is a commonly used hydrophilic and nonadsorbing polymer in biochemical and biotechnological applications. In the field of protein crystallography, PEG serves as one of the most widely used precipitating agents to obtain protein crystals for X-ray structural studies.[1] PEG is also used for studying macromolecular crowding effects in vitro.[2,3] These applications rely heavily on a universal and nonspecific attractive interaction or excluded volume effect which can be induced by PEG molecules.

The origin of PEG-induced attraction is qualitatively interpreted in terms of an entropy-driven depletion interaction that arises from the unbalanced osmotic pressure generated by the exclusion of polymer molecules from the volume between adjacent proteins. The polymer concentration determines the strength of interaction, whereas the range of interaction is controlled by both the polymer concentration and its radius of gyration, R_g, which is empirically calculated by $R_g = 0.02M_w^{0.58}$ with M_w being the polymer molecular weight.[4] The depletion interaction between particles (radius R) induced by polymer molecules was successfully predicted by the Asakura−Oosawa (AO) model in the colloid limit ($R > R_g$) and in dilute polymer concentration.[5] However, the AO model cannot be applied to the interpretation of the depletion interaction in the protein limit ($R < R_g$) and in the semidilute and concentrated regime over the crossover concentration, C_p^* (= $(M_w/44)^{-0.8}$). In this regime, polymer molecules cannot retain the spherical structure as represented by R_g, and they overlap one another and exhibit the network structure. Kulkarni et al.[6−8] have shown that protein interactions indicated as the osmotic second virial coefficient, B_2, were nonmonotonically changed with increasing concentrations of PEG 1000, 6000, and 12000 in lysozyme solutions, and these nonmonotonic behaviors were well described by the thermal polymer references interaction site model (PRISM) theory[9] which takes into account the effect of thermal polymer density fluctuations in depletion forces. A small-angle X-ray scattering study has also confirmed the reliability of the PRISM theory to predict the depletion attractions.[10]

Herein, we focus on protein rotational diffusion as a probe of this concentration-dependent microscopic behavior of PEG with high molecular weights ($R < R_g$) and the resulting effect on protein interactions. Rotational diffusion can be described from a movement of spatial orientation angle[11] and is known to be susceptible to the nature of the interaction potential at short-time and -spatial scales.[12] At the short-time regime, particle motion is affected by the presence of other nearby particles without the collision, and its rotational diffusion is changed with increasing particle concentration due to solvent-mediated hydrodynamic interactions.[13] An NMR relaxation study revealed that protein rotational diffusion was retarded by the long-range electrostatic interactions with increasing protein concentration.[14] In this context, the investigation on protein rotational diffusion in interacting systems is expected to be useful to further our understanding of protein interactions. In our previous study, we have demonstrated that the retardation of rotational diffusion of a fluorescein-labeled lysozyme molecule with increasing lysozyme concentrations (~20 mg/mL) well reflected the salt-induced attractive interactions which were induced depending on the salt type and

Received: June 6, 2011
Revised: August 31, 2011
Published: September 06, 2011

its concentration.[15] To avoid the undesirable effects for fluorescence anisotropy measurements, such as multiple light scattering, resonance energy transfer, and the reabsorption of emitted photon in concentrated protein solutions, we examined a small quantity of fluorescent-labeled lysozyme as a tracer molecule in native lysozyme solutions.

In this study, the effects of various concentrations and molecular weights (400, 1000, 6000, and 10000) of PEG on lysozyme interactions were characterized by applying the same procedure as we previously reported.[15] The results show the nonmonotonic changes in the interaction parameter, k_{rot}, as PEG concentration and M_w increases; the attractions are slightly increased in solutions of higher M_w of PEG when the solution approaches to the crossover concentration, C_p^*. We also examined the increase of physical mesh length by a temperature increase on the changes in the lysozyme rotational diffusion behavior and discussed the sensitivity of rotational diffusion to the long-range attractive interactions induced by PEG. Moreover, the validity of this approach was checked by comparison with the colloidal theory that treats the rotational diffusion and intermolecular interactions. The uniqueness of the protein rotational diffusion was also characterized.

EXPERIMENTAL METHODS

Protein and Chemicals. Hen egg white lysozyme, six times crystallized (M_w = 14 307, 99% purity) was purchased from Seikagaku Corporation. PEG with M_w ranging from 400 to 10 000 g/mol (PEG400 ∼ PEG10000), sodium chloride (NaCl), and fluorescein isothiocyanate isomer I (FITC, M_w = 389) were purchased from Sigma-Aldrich. All reagents were used without further purification.

Fluorescence Labeling. The covalent linking of FITC to the N-terminal amino group of lysozyme and the determination of the labeling stoichiometry were successfully performed as previously described.[15] The dye-to-protein ratio in the FITC-labeled lysozyme (F-lysozyme) was determined as 0.8:1 by absorbance measurements using the extinction coefficient of 2.64 mL mg^{-1} cm^{-1} at 280 nm for lysozyme[16] and the molar extinction coefficient of 68 000 M^{-1} cm^{-1} (pH 8.0) at 494 nm for FITC. F-lysozyme was then concentrated to the desired final concentration (∼30 mg/mL) by centrifugation with Centricon YM-3 (Amicon) after dialysis against 50 mM sodium acetate buffer at pH 4.6. Concentrated F-lysozyme was filtered with a 0.1 μm filter (Ultrafree-MC centrifugal filter device, Millipore) and kept frozen to −80 °C before use.

Sample Preparation. Lysozyme and PEG solutions were prepared separately by dissolving them in 50 mM sodium acetate buffer at pH 4.6 prepared with distilled water from a Milli-Q water purification system (Millipore) and then filtered through a 0.22 μm sterile filter (Millipore). A small aliquot of F-lysozyme prepared above was added into the lysozyme solution as a fluorescence tracer molecule with the final concentration of 0.03 mg/mL (∼2 μM) to avoid the undesirable fluorescence depolarization due to the resonance energy transfer between concentrated fluorescent molecules.[17] Calculated amounts of concentrated NaCl solution (4 M) were added to PEG solutions to adjust the solution ionic strength. Before fluorescence anisotropy measurements, these lysozyme (0−40 mg/mL of unlabeled lysozyme plus F-lysozyme) and PEG solutions were mixed at a ratio of 1:1 to give the required concentrations. Fluorescence measurements were performed at 20 ± 1 °C unless stated otherwise.

Fluorescence Anisotropy Measurements. Steady-state fluorescence anisotropy measurements were performed using a HITACHI 850 fluorescence spectrophotometer (Hitachi) equipped with two polarizers for excitation and fluorescence detection.

Time-resolved fluorescence anisotropy decay measurements were conducted using a time-correlated single-photon counting (TCSPC) method. The details of the experimental setup have been previously described.[15] In short, a 480 nm pulse at a repetition rate of 800 kHz generated by a mode-locked Ti:sapphire pulse laser and frequency doubler (Tsunami and model #3980 frequency doubler/pulse selector, Spectra-Physics) was used for excitation of the F-lysozyme. The vertically, $I_{VV}(t)$, and horizontally, $I_{VH}(t)$, polarized emission decays with vertically polarized excitation were detected on a microchannel plate-type photomultiplier (3809U-50, Hamamatsu Photonics) and accumulated in 2048 channels, with a time resolution of 11.8 ps/ch. Typically, $1-2 \times 10^4$ peak counts were collected. The instrument response function was decided by measuring the scattered light from a diluted polystyrene latex suspension (0.1 μm diameter). The G-factor was decided to be 1.40 by measuring the intensity ratio of the vertically, $I_{HV}(t)$, and horizontally, $I_{HH}(t)$, polarized emission components of the free FITC molecule with horizontally polarized excitation. For both steady-state and time-resolved measurements, fluorescence emission was detected at 520 nm.

Data Analysis of Fluorescence Anisotropy Measurements. Time-resolved anisotropy decays of vertical ($I_{VV}(t)$) and horizontal ($I_{VH}(t)$) components with vertically polarized excitation are given as follows[15,17]

$$I_{VV}(t) = \frac{1}{3} I(t)[1 + 2r(t)] \quad (1)$$

$$I_{VH}(t) = \frac{1}{3} I(t)[1 - r(t)] \quad (2)$$

where $I(t)$ and $r(t)$ are the total fluorescence intensity decay and fluorescence anisotropy decay, respectively, which can be described as a sum of exponentials. For relatively simple cases, the anisotropy decay can be described by a double exponential function, as shown below

$$r(t) = \beta_L \exp(-t/\phi_L) + \beta_S \exp(-t/\phi_S) \quad (3)$$

where ϕ_L represents the entire rotational correlation time of the protein and ϕ_S the rotational correlation time of fast segmental motion around the fluorophore. β_L and β_S are the pre-exponential terms related to the amplitude of each rotational motion, and the sum of them is the time-zero anisotropy, $\beta_L + \beta_S = r(0)$. The subscripts L and S denote the long- and short-time components, respectively. Anisotropy decays of F-lysozyme for all measurement conditions were fitted using this equation with maximum accuracy. Assuming a spherical shape of the protein molecule, the correlation time for the protein's entire rotation, ϕ_L, is converted to the rotational diffusion coefficient, D^0_{rot}, and is directly related to the hydrodynamic volume of protein, V, temperature, T, and viscosity of the solution, η, by the well-known Stokes−Einstein−Debye (SED) relationship

$$\phi_L = \frac{1}{6D^0_{rot}} = \frac{\eta V}{kT} \quad (4)$$

In addition, the freedom of the segmental mobility, f, is given from the relative amplitudes[18]

$$f = \frac{\beta_S}{\beta_L + \beta_S} \quad (5)$$

The $I_{VV}(t)$ and $I_{VH}(t)$ decay curves were analyzed globally by means of the nonlinear least-squares iterative convolution method based on the Marquart algorithm[19,20] to recover the intensity and anisotropy decay parameters. Diagnosis of the fitting adequacy was carried out using the statistical parameters such as the sigma value, the serial variance ratio (SVR), and plots of weighted residuals.

By definition, steady-state fluorescence anisotropy, r_{ss}, is given as follows and can also be calculated from an average of the anisotropy decay, $r(t)$, over the intensity decay, $I(t)$[17]

$$r_{ss} = \frac{I_{VV} - G\cdot I_{VH}}{I_{VV} + G\cdot 2I_{VH}} = \frac{\int_0^\infty I(t)r(t)\mathrm{d}t}{\int_0^\infty I(t)\mathrm{d}t} \quad (6)$$

where I_{VV} and I_{VH} are the steady-state vertical and horizontal fluorescence intensities against the vertical excitation, respectively. G is the polarization bias of the detection instrumentation equipped in the fluorescence spectrophotometer.

Interaction Parameter for Protein Rotational Motion. In a noninteracting system, i.e., at an infinitely dilute protein concentration, steady-state fluorescence anisotropy, r_{ss} (eq 6), is related to the rotational diffusion coefficient of protein, D^0_{rot}, and fluorescence lifetime, τ, according to the Perrin equation[21]

$$\frac{1}{r_{ss}} = \frac{1}{r_0}(1 + 6D^0_{rot}\tau) \quad (7)$$

where r_0 is the initial anisotropy decided only by the angular difference between the absorption and fluorescence transition moments.

Jullien et al. have expanded this equation to an interacting system and investigated the changes in rotational dynamics and intermolecular interactions of ribonuclease A for the initial step in its crystallization.[22] They anticipated that an apparent rotational correlation time, ϕ_{app}, in the interacting system would deviate from ideality in proportion to the protein concentration and introduced an empirical virial coefficient, α, for the rotational mobility. We extended their methodology as follows. The strength of protein interactions is generally characterized by the osmotic second virial coefficient, B_2, estimated mainly via optical scattering techniques (static light and small-angle X-ray scatterings). Meanwhile, B_2 is directly proportional to the interaction parameters estimated through dynamic light scattering (DLS) measurement of the translational diffusion coefficient of macromolecules, D_t,[23] and there is a reciprocal relationship between the rotational correlation time, ϕ, and the rotational diffusion coefficient, D^0_{rot} (eq 4). We, therefore, installed an interaction parameter, k_{rot}, associated with the rotational diffusion coefficient of protein following the case of the translational diffusion coefficient.[15]

At the region of the semidilute protein concentration, an empirical relation among an apparent rotational diffusion coefficient, D_{rot}, and the interaction parameter, k_{rot}, delineating the deviation from the ideality of protein solution behavior is given as

$$D_{rot} = D^0_{rot}(1 + k_{rot}[C]) \quad (8)$$

Table 1. Rotational Correlation Time, ϕ_L, of F-Lysozyme at 0.2 M NaCl with and without 0.01 g/mL of PEG10000[a]

	rotational correlation time (ns) for entire rotation, ϕ_L	
lysozyme concentration (mg/mL)	0.2 M NaCl	+ PEG10000 0.01 g/mL
0.03	6.34 ± 0.20	7.54 ± 0.14
1	6.37	7.27 ± 0.10
3	7.16	7.41
5	7.05 ± 0.32	8.05 ± 0.69
10	7.76 ± 0.27	8.43 ± 0.18
12.5	7.19	9.31
15	7.53 ± 0.09	8.83
20	8.08 ± 0.02	10.00

[a] Experimental errors obtained from the repeated experiment are also shown.

In this case, an apparent fluorescent anisotropy value, r_{app}, measured by the steady-state method, is expressed as follows

$$\frac{1}{r_{app}} = \frac{1}{r_0}(1 + 6D_{rot}\tau) \quad (9)$$

Dividing eq 9 by eq 7 and combining it with eq 8, we obtained the following equations, by which the r_{app} value measured was linked to the interaction parameter, k_{rot}

$$\frac{r_{ss}}{r_{app}} = (1 + l[C]), \qquad l = k_{rot}\left(1 - \frac{r_{ss}}{r_0}\right) \quad (10)$$

Utilizing the above relationships, k_{rot} values under the various conditions can be estimated from the dependence of r_{app} and D_{rot} on the protein concentration (0−20 mg/mL), which are measured by steady-state and time-resolved fluorescence anisotropy measurements, respectively. If k_{rot} is negative, the net interaction has an attractive direction, and D_{rot} becomes smaller than D^0_{rot}, and vice versa.

RESULTS AND DISCUSSION

Time-Resolved Measurements. The time-resolved fluorescence measurements were performed for F-lysozyme in two different conditions, 0.2 M NaCl with and without 0.01 g/mL of PEG10000 (R_g = 4.18 nm). The fluorescence intensity, $I(t)$, and anisotropy, $r(t)$, decays measured in these conditions could be well fitted to the triple and double exponential kinetics by applying the global analysis procedure.[19,20] Table 1 shows the protein concentration dependence of the entire rotational correlation time, ϕ_L, of F-lysozyme.

According to eq 4, the ϕ_L value is converted to the apparent rotational diffusion coefficient, D_{rot}. Figure 1 illustrates the plot of D_{rot} against the lysozyme concentration at two different conditions mentioned above. Linear fitting of each D_{rot} plot gives the intercept value corresponding to the rotational diffusion coefficient at an infinite dilution, D^0_{rot}. Using the D^0_{rot} values, the hydrodynamic radius of lysozyme was calculated to be 1.83 nm on the solution viscosity (η = 1.04)[24] and 293 K in the absence of PEG10000. This value is in between the equivalent spherical radius values of a lysozyme monomer, 1.72 and 1.9 nm, measured from the crystallographic structure and DLS,[25] respectively.

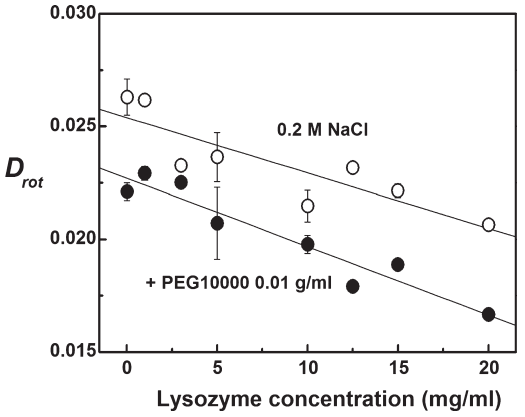

Figure 1. Plot of D_{rot} versus the lysozyme concentrations. D_{rot} was calculated using eq 4 from the entire rotational correlation time, ϕ_L. Interaction parameter, k_{rot}, was directly estimated from the slope and intercept values (eq 8).

Figure 1 shows the small differences in the slopes and intercept values obtained for lysozyme solution with and without PEG10000. Using eq 8, for the interaction parameter, k_{rot}, values of -0.97×10^{-2} and -1.34×10^{-2} mL/mg were obtained in the absence and presence of PEG10000, respectively. This fact indicates that the slowdown of the rotational diffusion reflects PEG-induced long-range attractive forces. However, the differences in the ϕ_L values at constant lysozyme concentration are relatively small as seen in Table 1. It may be attributed to the practical difficulty in directly measuring protein rotational diffusion coefficients with a high degree of accuracy by the time-resolved technique.

Among the results from the time-resolved measurements, except for the slight difference in ϕ_L (Table 1) and ϕ_S, we could confirm that other changes in the intensity decay and anisotropy decay parameters are negligible. In addition, the uncertainty regarding the measurement of a shorter rotational correlation time (ϕ_S < 500 ps) and the freedom of the lysozyme N-terminal motion, f (eq 5), precludes any definite conclusions of how PEG molecules affect the segmental flexibility of F-lysozyme in solution. On the basis of the definition of the steady-state anisotropy, r_{ss} (eq 6), we calculated r_{ss} from the parameters obtained by time-resolved measurements and estimated the contribution of the entire and segmental depolarizing motion on the r_{ss} values, respectively. As a result, the contribution from the fast segmental motion around the N-terminus of F-lysozyme was considerably small (<5%). Therefore, we can reason that the steady-state measurement is sufficient to investigate the entire rotational motion and its changes against surrounding environments and protein interactions. In this way, the validity of steady-state measurements to estimate k_{rot} is demonstrated (described below).

Effects of PEG10000 at Various Ionic Strengths. Figure 2a illustrates the result of steady-state fluorescence anisotropy measurements as a plot of $1/r_{app}$ versus the lysozyme concentration in the presence of different concentrations of PEG10000 and NaCl. From eq 10, linear fitting of each plot gives the slope and the intercept value, producing the interaction parameter for protein rotational diffusion, k_{rot} (Figure 3). A time-zero anisotropy ($r(0)$) value of 0.326, obtained from time-resolved anisotropy measurement, was used for r_0 in eq 10. The result suggests that, in the absence of PEG10000, the negative slope is steepened with increasing concentration of NaCl from 0 to 0.2 M, indicating attractive interactions due to the screening of electrostatic repulsion.

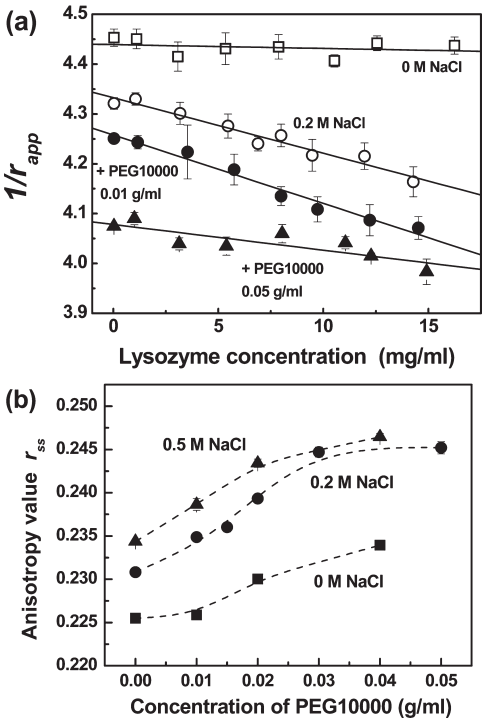

Figure 2. (a) Effects of increasing NaCl and PEG10000 concentrations on apparent fluorescence anisotropy, r_{app}, of fluorescein-tagged lysozyme. The NaCl and PEG10000 concentrations are indicated near the line obtained by the linear fitting of each plot. (b) The r_{ss} values at an infinitely dilute protein concentration plotted against the PEG10000 concentrations. All data were obtained from the intercept value of linear fitting of the plot of $1/r_{app}$ in 0 M NaCl (■), 0.2 M NaCl (●), and 0.5 M NaCl (▲).

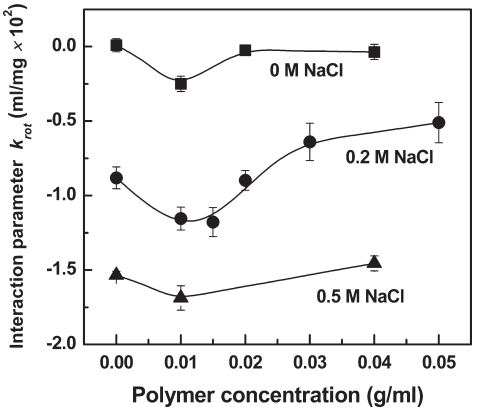

Figure 3. Interaction parameter, k_{rot}, as a function of PEG10000 concentration. The lines are drawn to guide the eye. NaCl concentration is indicated near the line. All measurements were performed at 20 °C.

These results also suggest that the averaged rotational diffusion of F-lysozyme is slowed down with increasing protein concentrations. Addition of 0.01 g/mL of PEG10000 causes a slight change in the slope of $1/r_{app}$ toward the negative direction, while a further increase in PEG10000 concentration (~0.05 g/mL) that is well beyond the crossover concentration from dilute to semidilute (C_p^* = 0.013 g/mL) at 0.2 M NaCl results in the gently inclined slope. The r_{ss} values corresponding to the reciprocal of intercept values is increased with increasing PEG

and NaCl concentrations (Figure 2b). In the absence of protein interactions, the r_{ss} values obtained from the intercept value monotonically grow with increasing polymer concentrations up to 0.03 g/mL (>C_p*) and seem to be constant at higher polymer concentrations.

Variation of k_{rot} values with increasing both PEG10000 and NaCl concentrations is depicted in Figure 3. Qualitatively, nonmonotonic changes in k_{rot} are observed, and the attractive minimum is located in the vicinity of the crossover concentration, C_p*, for all ionic strengths (0, 0.2, and 0.5 M of NaCl), which is similar to the change of the second virial coefficient.[6−8] The nonmonotonic behavior is relatively weak at 0 M NaCl where the electrostatic repulsion governs protein interactions, and it is diminished to a certain degree at 0.5 M NaCl where the attractive interactions due to the screening of the electrostatic repulsion by added salt molecules are dominant. The decrease in the k_{rot} values (the increase of a degree at which the protein rotational diffusion is slowed down with increasing protein concentration) that reflect an increase in the intermolecular attraction is clearly observed at 0.01−0.015 g/mL of PEG10000 in the case of 0.2 M NaCl. Although the differences observed in the changes of the slope of $1/r_{app}$ between the absence and presence of PEG10000 are considerably smaller when comparing to the effects of NaCl between 0 and 0.2 M (Figure 2a), long-range depletion attractions induced by PEG10000 (R_g = 4.18 nm > R = 1.7 nm) can be clearly monitored thorough the changes in the degree of the retardation of F-lysozyme rotational motion.

In contrast, at higher concentrations of PEG10000 (0.03−0.05 g/mL) that are above the crossover concentration, C_p*, the protein interactions vary toward the repulsive interactions (k_{rot} increases again) (Figure 3). In this regime, the flexible polymer molecules change their own conformation in solution and cannot hold the spherelike structure whose radius is represented as R_g, and a dense network-like structure is formed around protein molecules, leading to the decrease in depletion attraction. Experimental[26] and simulation studies[27] indicated the presence of weak attractive interactions between polymer and protein molecules probably due to hydrophobic effects. The adsorption of polymer segments on protein molecules was then suggested to promote the repulsive interaction between protein molecules.[7] Our results are virtually in good agreement with those of Kulkarni et al. measuring the normalized osmotic second virial coefficient, B_2/B_2^{HS}.[6−8]

Effects of Various M_w and Concentrations of PEG. We measured the interaction parameter, k_{rot}, in the presence of different M_w (400, 1000, 6000, and 10000) and concentrations of PEG at a constant ionic strength of 0.2 M NaCl. The results are shown in Figure 4. For PEG6000 (R_g = 3.11 nm), the nonmonotonic change in k_{rot} with the minimum occurring at near C_p* = 0.02 g/mL is observed as in the case of PEG10000 (Figure 3), and the magnitude of induced attractive interactions is smaller than that by PEG10000. The nonmonotonic behavior is progressively weakened when the M_w of PEG decreases and completely disappears for PEG400 which has a smaller gyration radius (R_g = 0.65 nm) than that of lysozyme. As regards the increase in k_{rot} with increasing polymer concentration (>C_p*), no specific trends depending on PEG molecular weight are observed.

Temperature Dependence of the Interaction Parameter. According to the PRISM theory,[9] when the temperature increases toward the spinodal temperature, T_S, and the PEG solution approaches phase separation, the physical mesh length, ξ_ρ, which determines the spatial range of depletion interactions,

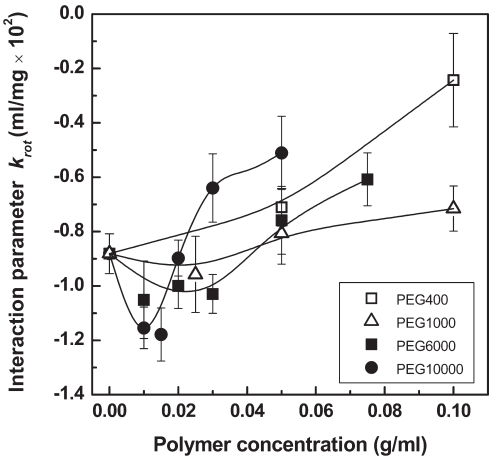

Figure 4. Interaction parameter, k_{rot}, for the lysozyme rotational diffusion as a function of concentration of PEG400, 1000, 6000, and 10000. Solution ionic strength is fixed at 0.2 M in 50 mM sodium acetate buffer. The symbol represents the experimental data, and the lines are to guide the eye.

Table 2. Temperature Dependence of the Interaction Parameter, k_{rot} (with Errors in Linear Fitting Analysis), of F-Lysozyme at Fixed Ionic Strength of 0.2 M with and without 0.01 g/mL of PEG10000

temperature (°C)	PEG10000 conc. (g/mL)	$k_{rot} \times 10^2$ (mL/mg)
45	0	−0.303 ± 0.041
	0.01	−0.263 ± 0.042
35	0	−0.253 ± 0.052
	0.01	−0.367 ± 0.109
25	0	−0.431 ± 0.052
	0.01	−0.707 ± 0.043
20	0	−0.881 ± 0.073
	0.01	−1.154 ± 0.077

increases. Kulkarni et al.[7] have demonstrated that the increase in temperature resulted in the decrease in B_2/B_2^{HS}, i.e., the increase in the attractive interaction, at a fixed concentration of PEG10000, $C_p < C_p$* (seen in Figure 9 of ref 7). We here investigated the effect of temperature and resulting structural changes of polymer solution on protein interactions from the behavior of protein rotational diffusion. Table 2 shows the k_{rot} values obtained at four temperatures, and their difference, $\Delta k_{rot} = k_{rot}(C_p = 0.01) - k_{rot}(C_p = 0)$, is plotted in Figure 5 as a function of temperature. The difference of k_{rot} with and without PEG10000 tapers off with increasing temperature. At 45 °C, the difference has totally vanished, indicating that the increase in the spatial range of depletion interaction is not reflected in the changes of F-lysozyme rotational diffusion with increasing protein concentrations. These results are opposite to those of Kulkarni et al.[7] who showed by measuring B_2 that PEG-induced long-range attractive interaction between lysozyme molecules increased with increasing temperature. On the basis of the SED relation for rotational diffusion (eq 4), a temperature increase gives rise to enhanced thermal energy of protein molecules, resulting in the enhanced rotational diffusivity, i.e., the increase of the rotational diffusion coefficient, D_{rot}. It is therefore probable that the enhanced rotational diffusion of the protein due to the increased thermal

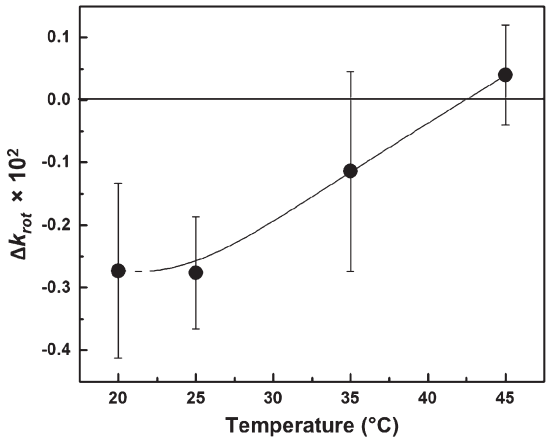

Figure 5. Temperature dependence of $\Delta k_{rot} = k_{rot}(C_p = 0.01) - k_{rot}(C_p = 0)$. C_p is PEG10000 concentration (g/mL).

energy makes the protein rotational diffusion less sensitive to the long-range attractive interaction when temperature increases, although protein attractive interactions are totally increased as reflected in the changes of B_2.[7] Because rotational diffusion is driven by tangential forces exerting a torque on the protein, it has much shorter time- and spatial-scales than those of translational diffusion commonly measured for B_2 determination. The driving force for translational diffusion, on the other hand, is the osmotic pressure closely linked with the concentration fluctuation in an interacting system. It would be likely that these differences in driving forces and spatiotemporal scales lead to the difference observed for the temperature effect on k_{rot} and B_2.

Comparison to the Colloidal Theory for Rotational Diffusion. Rotational diffusion in suspensions of particle has hitherto been investigated mainly in the field of colloidal physics. In this section, we evaluated the changes in D_{rot} with increasing protein concentrations in the absence and presence of PEG10000 (shown as above) in the light of colloidal physics theories. Prior to doing this, it is necessary to estimate the time scale where the rotational diffusion occurs. In a short time regime, the particle can move without the collision of neighboring particles, whereas in a long time regime, the trajectory of particle motion is determined by collisions with other particles. The characteristic collision time, τ_{col}, is given by the Smoluchowski equation[13]

$$\tau_{col} = \left[\frac{4\pi k_B T}{6\pi\eta}(r_p + r_c)\left(\frac{1}{r_p} + \frac{1}{r_c}\right)\theta\right]^{-1} \quad (11)$$

where r_p and r_c are the hydrodynamic radii of the protein and the cosolute; θ is the volume fraction of particles in solution which is calculated by $\theta = N\Omega/V$; N is the number of molecules; Ω is the effective volume of a single molecule; and V is the solution volume. The time scale can be estimated by comparing the interval between collisions with the characteristic time of translational free Brownian motion, τ_{trans}, which can be defined as the time for which the root-mean square displacement is the same as the particle radius. The short time regime occurs when $\tau_{col} \gg \tau_{trans}$, while when $\tau_{col} \ll \tau_{trans}$ the long time regime occurs. To estimate it, Bernado et al. supposed the instructive equation using the ratio of radii, $\lambda = r_p/r_c$[13]

$$\frac{\tau_{trans}}{\tau_{col}} \approx \theta F(\lambda) \text{ where } F(\lambda) = \frac{1}{2}(1 + \lambda)(1 + \lambda^{-1})\lambda^3 \quad (12)$$

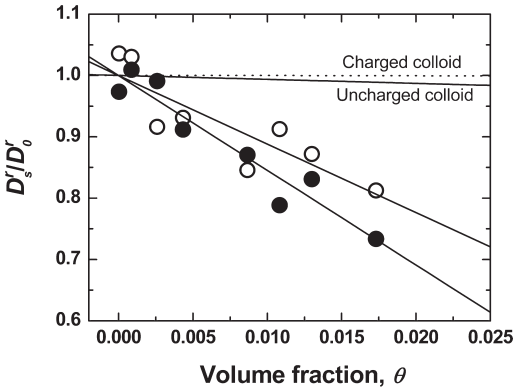

Figure 6. Replot of D_{rot} as the normalized rotational diffusion coefficient at short-time regime, D_s^r/D_0^r, with increasing particle volume fraction, θ. Open circle (○) represents the data obtained for the absence of PEG10000 and closed circle (●) the presence of 0.01 g/mL of PEG10000. Black line describes the theoretical models (solid line for uncharged colloid, dotted line for charged colloid molecules).

On the basis of eq 12, this ratio was calculated for our system consisting of F-lysozyme (the protein of interest), lysozyme (cosolute-1), and PEG10000 (cosolute-2), and τ_{trans}/τ_{col} was 0.0085 and 0.0317 in the case of F-lysozyme and 20 mg/mL of lysozyme ($\lambda = 1$) and F-lysozyme and 0.01 g/mL of PEG10000 ($\lambda = 0.415$), respectively. Therefore, the time regime we focused on can be defined as the short time regime.

As mentioned above, in the short-time regime, the particle moves in an unchanging equilibrium configuration of neighboring particles. For the uncharged identical hard sphere, the short time rotational diffusion coefficient, D_{short}^r, is retarded with increasing surrounding particle volume fraction described as follows[28]

$$D_{short}^r = D_0^r(1 - 0.6310\theta - 0.726\theta^2) \quad (13)$$

where the first term (−0.6310) represents the contribution from two-body interactions and is analogous to our interaction parameter, k_{rot}. The second one (−0.726) represents three-body interactions.[12] Then, considering an identically charged sphere, its rotational diffusion is less affected by crowding due to that electrostatic repulsion increases the distance between the nearest particles. Thus, the rotational diffusion shows a nonlinear dependency on θ. For such a case[29]

$$D_{short}^r = D_0^r(1 - 1.3\theta^2) \quad (14)$$

Figure 6 shows the comparison between the colloidal theory (eqs 13 and 14) and the results obtained for the lysozyme−PEG system as the replot of D_s^r/D_0^r versus the volume fraction of particle, θ (protein and colloid). Compared to the colloidal theory, the decreases of D_s^r/D_0^r (the retardation of the rotational diffusion) have considerably larger negative slopes (−11.18 for 0.2 M NaCl and −15.44 for 0.2 M NaCl plus 0.01 g/mL of PEG10000). Koenderink et al. showed that the screening of electrostatic repulsion by the addition of salts gives rise to a slow down of the colloid rotational diffusion compared to that predicted by the theory.[12] However, the deviation of the case for the rotational diffusion of lysozyme from the theory is considerably larger than their results. Furthermore, our results cannot be fitted with a quadratic function which describes the rotational diffusion of a charged sphere (eq 14) despite that the lysozyme molecule has a large positive charge at pH. 4.6. Our results indicate that, in the short-time regime where the hydrodynamic interaction is attributed to the potent factor affecting

the diffusion of particles, the rotational diffusion of F-lysozyme molecules is substantially slowed down with increasing volume fraction of lysozyme molecules. Possibly, the shape complementarity and the anisotropic charge distribution of protein molecules have a large impact on the sensitivity of protein rotational diffusion for the interaction such as hydrodynamic and electrostatic interactions without the collision. Furthermore, from the comparison with the colloidal theory, it can also be confirmed that the long-range attractive interaction induced by PEG is reflected in further a slow down of the protein rotational diffusion.

CONCLUSIONS

We here characterized PEG-induced depletion interactions by studying protein rotational diffusion using the fluorescence anisotropy technique and interaction parameter, k_{rot}. Earlier studies by Kulkarni et al. have demonstrated the nonmonotonic behavior of the PEG-induced depletion interaction through the measurement of B_2 for lysozyme solutions.[6−8]

Our experimental results reveal that, at the polymer concentrations close to C_p^* and 0.2 M NaCl, long-range attractive protein interactions induced by PEG10000 and 6000 ($R_g > R$) are characterized by the decreases in k_{rot} (Figures 3 and 4). This indicates the increase of a degree at which the protein rotational diffusion is slowed down when protein concentration is increased (Figures 1 and 2a). Further increase of PEG concentration ($>C_p^*$) results in the increase in the k_{rot} values, indicative of repulsive interactions. This nonmonotonic behavior of k_{rot} disappears in the case of lower molecular weights of PEG (Figure 4). Our results described above, except for the temperature dependence of k_{rot}, are in good agreement with measurements of B_2 for lysozyme−PEG solutions by Kulkarni et al.[6−8] The osmotic second virial coefficient, B_2, generally represents averaged interaction forces between protein molecules, whereas k_{rot} values presented here can be obtained from the changes in protein rotational diffusion being affected by tangential forces exerting a torque on the protein.[11] However, it is not clear how the averaged force has an impact on the tangential force. From the colloidal theory, rotational diffusion is known to be sensitive to the short-range interactions.[12] Protein interactions consist of noncovalent forces including van der Waals, electrostatic, hydrophobic, and hydrodynamic interactions which have the short-range nature, and the long-range depletion forces are induced by polymer such as PEG. Therefore, it would be reasonable that the integration of such forces affects the behavior of protein rotational diffusion in response to various solution conditions modified by additives. Thus, the relatively weak and long-range depletion attractions induced by adding PEG with higher molecular weights at a constant ionic strength may hinder the protein rotational diffusion to some extent, resulting in the comparatively smaller decrease of k_{rot} values than that by adding salt molecules in polymer-free conditions (shown in Figure 3). In Figure 6, the slight slow down of the protein rotational diffusion due to the addition of PEG10000 can also be observed in the comparison with the colloidal theory which connects the particle rotational diffusion and interactions.[28,29] Precise interpretation on the mutual relationship between B_2 and k_{rot}, however, requires further investigations and theoretical considerations on the protein rotational diffusion which has shorter spatial and temporal scales compared to translational diffusion.

The lysozyme we used here is the model protein for studying protein crystallization and interactions due to its inherent rigidity and high commercial availability in the purest form. The validity of using the steady-state fluorescence anisotropy to monitor the entire rotational dynamics of lysozyme is based on the substantially small contribution from the N-terminus segmental mobility on the r_{ss} values. However, to expand this approach for highly flexible proteins such as the intrinsically disordered proteins,[30] the differentiation of the entire and the fast segmental rotational correlation times by using a time-resolved technique will be required to clearly describe the effect of protein interactions on its rotational diffusion.

AUTHOR INFORMATION

Corresponding Author

*E-mail: enish@brs.kyushu-u.ac.jp. Phone/Fax: +81-92-642-4425.

REFERENCES

(1) McPherson, A. *Crystallization of Biological Macromolecules*; Cold Spring Harbor Laboratory Press: New York, 1999.
(2) Kozer, N.; Kuttner, Y. Y.; Haran, G.; Schreiber, G. *Biophys. J.* **2007**, *92*, 2139–2149.
(3) Kuttner, Y. Y.; Kozer, N.; Segal, E.; Schreiber, G.; Haran, G. *J. Am. Chem. Soc.* **2005**, *127*, 15138–15144.
(4) Kawaguchi, S.; Imai, G.; Suzuki, J.; Miyahara, A.; Kitano, T. *Polymer* **1997**, *38*, 2885–2891.
(5) Asakura, S.; Oosawa, F. *J. Chem. Phys.* **1954**, *22*, 1255–1256.
(6) Kulkarni, A. M.; Chatterjee, A. P.; Schweizer, K. S.; Zukoski, C. F. *Phys. Rev. Lett.* **1999**, *83*, 4554–4557.
(7) Kulkarni, A. M.; Chatterjee, A. P.; Schweizer, K. S.; Zukoski, C. F. *J. Chem. Phys.* **2000**, *113*, 9863–9873.
(8) Kulkarni, A. M.; Zukoski, C. F. *J. Cryst. Growth* **2001**, *232*, 156–164.
(9) Chatterjee, A. P.; Schweizer, K. S. *J. Chem. Phys.* **1998**, *109*, 10464–10476.
(10) Vivares, D.; Belloni, L.; Bonnete, F. *Eur. Phys. J.* **2002**, *9*, 15–25.
(11) Tanford, C. *Physical Chemistry of Macromolecules*; Wiley: New York, 1961.
(12) Koenderink, G. H.; Lettinga, M. P.; Philipse, A. P. *J. Chem. Phys.* **2002**, *117*, 7751–7764.
(13) Bernado, P.; Garcia de la Torre, J.; Pons, M. *J. Mol. Recognit.* **2004**, *17*, 397–407.
(14) Krushelnitsky, A. *Phys. Chem. Chem. Phys.* **2006**, *8*, 2117–2128.
(15) Takahashi, D.; Nishimoto, E.; Murase, T.; Yamashita, S. *Biophys. J.* **2008**, *94*, 4484–4492.
(16) Aune, K. C.; Tanford, C. *Biochemistry* **1969**, *8*, 4579–4585.
(17) Lakowicz, J. R. *Principles of Fluorescence Spectroscopy*, 2nd ed.; Kluwer Academic/Plenum Publishers: New York, 1999.
(18) Nishimoto, E.; Yamashita, S.; Szabo, A. G.; Imoto, T. *Biochemistry* **1998**, *37*, 5599–5607.
(19) Willis, K. J.; Szabo, A. G. *Biochemistry* **1989**, *28*, 4902–4908.
(20) Zuker, M.; Szabo, A. G.; Bramall, L.; Krajcarski, D. T.; Selinger, B. *Rev. Sci. Instrum.* **1985**, *56*, 14–22.
(21) Weber, G. In *Fluorescence and Phosphorescence Analysis*; Hercules, D. M., Ed.; Interscience: New York, 1996; pp 217−240.
(22) Crosio, M. P.; Jullien, M. *J. Cryst. Growth* **1992**, *122*, 66–70.
(23) Zhang, J.; Liu, X. Y. *J. Chem. Phys.* **2003**, *119*, 10972–10976.
(24) Fredericks, W. J.; Hammonds, M. C.; Haward, S. B.; Rosenberger, F. *J. Cryst. Growth* **1994**, *141*, 183–192.
(25) Muschol, M; Rosenberger, F. *J. Chem. Phys.* **1995**, *103*, 10424–10432.
(26) Abott, N. L.; Blankschtein, D.; Hatton, T. A. *Macromolecules* **1992**, *25*, 3932–3941.
(27) Bedrov, D.; Penky, M.; Smith, G. D. *J. Phys. Chem. B.* **1998**, *102*, 10318–10323.
(28) Cichocki, B.; Ekiel-Jezewska, M. L.; Wajnryb, E. *J. Chem. Phys.* **1999**, *111*, 3265–3273.
(29) Watzlawek, M.; Nagele, G. *Phys. A* **1997**, *235*, 56–74.
(30) Dyson, H. J.; Wright, P. E. *Nat. Rev. Mol. Cell Biol.* **2005**, *6*, 197–208.